BMC Plant Biology

RESEARCH

Open Access

Genome-wide identification of the *AcBAM* family in kiwifruit (*Actinidia chinensis* cv. Hongyang) and the expression profiling analysis of *AcBAMs* reveal their role in starch metabolism

Xuchen Gong[1,2], Mengfei Lin[1,2], Jie Song[3], Jipeng Mao[1,2], Dongliang Yao[1], Zhu Gao[1,2*] and Xiaoling Wang[1,2*]

Abstract

After analyzing a high-quality 'Hongyang' genome, we identified 17 *AcBAMs*. Comprehensive bioinformatics were performed to elucidate the properties and evolutionary relationships of these genes. Our analysis revealed that most *AcBAMs* retained conserved active sites (e.g., Glu186 and Glu380) and exhibited similar structural properties. Phylogenetic and collinearity analyses grouped the genes into three main clusters, with segmental and tandem duplications contributing to their expansion. Expression profiling showed that *AcBAM5* and *AcBAM13* were most highly expressed during postharvest storage and were strongly induced by ABA signal. Silencing these genes led to a significant increase in starch content, suggesting their key role in starch degradation. Promoter analysis identified cis-elements related to ABA signal and cold response in the *AcBAM* family, and the expression of *AcBAM* genes was influenced by ABA and low-temperature treatments, with specific genes showing significant responsiveness.

Background Kiwifruit (*Actinidia chinensis* cv. Hongyang) is a perennial woody fruit tree highly valued for its rich nutritional profile and high vitamin C content. The postharvest ripening process, characterized by starch degradation into soluble sugars, significantly influences the fruit's flavor and texture. β-amylase (BAM) has been proven to be one of the key enzymes catalyzing starch degradation, but which *BAM* genes are involved and how to participate in this process in kiwifruit still need to be clarified.

Conclusion In the study, we identified a total of 17 *AcBAM* genes. The expansion of *AcBAMs* in kiwifruit was mainly due to segmental duplication events, and some of their catalytic residues were mutated, potentially leading to a loss of biological activity. The expression patterns of *AcBAMs*, along with VIGS data, suggest that *AcBAM5* and *AcBAM13* respond to ABA signals and promote starch degradation. Our findings provide valuable insights into the regulatory mechanisms of BAM genes in kiwifruit and highlight their importance in starch metabolism and fruit ripening.

Keywords Kiwifruit, Genome-wide identification, *AcBAM*, Starch degradation, Transcriptome analysis, ABA treatment, Low-temperature treatment

*Correspondence:
Zhu Gao
jxaugz2008@126.com
Xiaoling Wang
WangXL_JXAS@163.com
Full list of author information is available at the end of the article

Introduction

Kiwifruit (*Actinidia*) is a perennial woody fruit tree belonging to the Actinidiaceae family. Known for its juicy, fresh, and sweet fruit, kiwifruit is highly valued worldwide due to its rich nutritional profile, particularly its high vitamin C content. As of 2023, the global cultivation area for kiwifruit has exceeded 286 thousand hectares, with production surpassing 4.5 million tons and continuing to increase annually [1]. Nowadays, the kiwifruit industry has become a vital economic contributor in numerous countries and regions. With the increase in kiwifruit production, consumer demands for the quality of kiwifruit have intensified, prompting ongoing breeding efforts to develop new kiwifruit varieties. 'Hongyang' (*Actinidia chinensis* cv. Hongyang) is a recently bred cultivar known for its red flesh trait [2]. It is characterized by high vitamin C content and high T/A ratio, and the fruit's pulp near the core exhibits a light red hue [3]. 'Hongyang' kiwifruit usually begins to bear fruit in late April. During fruit development, kiwifruit accumulates a diverse array of organic substances such as soluble sugars, organic acids, polyphenols, and flavonoids [4]. These organic substances are also key sources helping to shape kiwifruit's unique flavor. Among these substances, starch assumes a critical role as a major organic compound amassed during kiwifruit development. The content of starch keeps increasing progressively since the fruit volume begins to expand and reaches its peak at the harvest period [5]. At this stage, the starch content of kiwifruit can reach over 40% of the total dry matter content. Therefore, starch is also regarded as an important marker for measuring whether kiwifruit meets the harvest standard [6].

After harvest, kiwifruit will undergo a post-ripening process due to its respiratory climacteric characteristics. During this process, kiwifruit experiences vigorous metabolic activity, with the fruit suddenly softening and the organic acid content decreasing [7]. The large amount of starch accumulated during the kiwifruit development stage also rapidly degrades and converts into small molecule soluble sugars such as glucose, fructose, and sucrose [8, 9]. Numerous enzymes are involved in the degradation of the starch process: glucose water dikinase (GWD) and phospholucan water dikinase (PWD) can damage the starch granules, exposing starch to the cytoplasm [10–12]; Subsequently, phytolucan phospholipase (SEX) hydrolyzes the phosphate groups on the starch chain, which facilitates the rapid hydrolysis of starch by amylase [13–15]; Finally, by α-Amylase and β-Amylase (BAM) completely hydrolyzes starch into glucose and maltose, which are further converted into other soluble sugars, forming the fresh and sweet taste of kiwifruit during its edible period [16–18].

α-amylase and β-amylase participate in the last step of starch hydrolysis and are generally considered as the rate-limiting enzymes in the process of starch degradation. Among them, β-amylase has no ability to hydrolyze α-1,6-glycosidic bond, and can only hydrolyze amylose or amylopectin to β-extreme dextrin. β-amylase has been proven to be the key enzyme for starch degradation in fruits such as mangoes and bananas during the postharvest storage [19, 20]. Studies in white clover, wheat, and citrus have shown that, β-Amylase can positively regulate plant resistance to stress by hydrolyzing starch [21]; The study found that the enzyme activity of α-amylase is higher during the development of kiwifruit, while both the gene expression level and the enzyme activity of β-Amylase increases rapidly during the postharvest period, indicating that starch hydrolysis during the kiwifruit storage is mainly caused by β-amylase, but its underlying molecular mechanisms are remain to be cleared [22].

Previous studies have identified the *BAM* gene family according to the genome of 'Red5'; however, due to the incompleteness of the Red5 genome and the lack of gene annotation, only 12 *BAM* genes have been identified [23]. In this study, to further investigate how β-amylose is involved in starch degradation in kiwifruit fruit, we used a high-quality and complete 'hongyang' genome to identify a total of 17 *AcBAM* genes in kiwifruit. A comprehensive study of *AcBAM* genes' Physical and chemical properties, the advanced structure of protein, phylogenetic analysis, and collinearity analysis was done via detailed bioinformatics analysis. Then we analyzed its expression level in kiwifruit during storage by performing a high throughput transcriptome sequencing. Furthermore, we verified the gene function through the VIGS experiment to provide a theoretical basis for subsequent research on starch metabolism in kiwifruit. This study will provide helpful insights for future investments about the mechanisms of which kiwifruit *BAM* gene family members regulate starch degradation during postharvest storage.

Materials and methods

Plant material and treatment

Kiwifruit (*Actinidia chinensis* cv. Hongyang) samples were collected from Fengxin County Doctor Kiwifruit Base, Yichun City, Jiangxi Province, China (E114°45', N28°34'). Fruit with uniform size was harvested at 180 d after pollination and immediately transported to Jiangxi Academy of Science.

Fruit was divided into three groups to perform different experiments. To analyze the expression of *AcBAMs* during storage, one group fruit was stored at 20 ℃ and was sampled every 4 d. Half of the fruits in another group

were treated with 500 ng/ul ABA solution, and the other half were treated with $_{dd}H_2O$ to explore whether *AcBAMs* were induced by ABA. Then the fruit was stored at 20 ℃ and sampled at 0 h, 9 h, 18 h, 36 h, and 72 h, respectively. One-third of the fruits in the last group were stored at 5 ℃, one-third at 15 ℃, and one-third at 25 ℃, and air circulation was ensured. The samples were collected at 0 h, 24 h, 48 h, 96 h, 8 d, and 15 d after storage to study the effect of temperature on the expression of *AcBAMs*. All samples were rapidly frozen with liquid nitrogen and stored at -80 ℃ for the next analysis. Three biological replicates were performed for each experiment.

Identification of BAM family genes in 'Hongyang' kiwifruit genome

To identify the *BAM* family members in 'Hongyang' Kiwifruit, we followed a three-step process:

1. Prediction of conserved domains: We predicted the conserved domains of nine *BAM* family genes in Arabidopsis using HMMER Search (https://www.ebi.ac.uk/Tools/hmmer/search/hmmscan). We confirmed the Pfam of Glyco_hydro_14 (PF01373) as the conserved domain of the glycosidase superfamily and downloaded the corresponding HMMER model from the same site. Using the newly published 'Hongyang v3.0' [24] genome (https://kiwifruitgenome.org/), protein sequence, and annotation data, we utilized HMMER (v11.0) software (http://hmmer.org/download.html) to identify *BAM* family genes. The 'hmmbuild' command in HMMER was used to create the SEED file in Stockholm format, and 'hmmsearch' was applied to identify potential *BAM* genes in the whole-genome protein sequence file, with the e-value cutoff set to 0.0001 [25].
2. Sequence Similarity Search: We conducted a local BlastP search to compare the Fasta-format SEED file with the whole-genome protein sequence file of Kiwifruit. Potential *BAM* genes were identified based on sequence similarity [26].
3. Validation of Candidate Sequences: To verify the reliability of these candidate sequences, we used the CDD-batch tool (https://www.ncbi.nlm.nih.gov/cdd) and SMART (http://smart.embl-heidelberg.de/) to confirm each candidate protein as a member of the *BAM* family. We identified a total of 17 *BAM* family genes, naming them *AcBAM1* – *AcBAM17* based on their e-values from the HMMER search process [27].

Analysis of physical and chemical properties of AcBAMs

ExPASy online resources were utilized to predict various physical and chemical parameters of the kiwifruit BAM protein, including molecular weight (MW), theoretical isoelectric point (pI), grand average hydropathicity (GRAVY), instability index, and aliphatic index. The SOPMA server was employed to analyze the secondary structure of the protein sequences for the 17 AcBAMs and determine the proportion of different secondary structures. For tertiary structure prediction, we used the SWISS-PROT to build the tertiary structure model for AcBAMs and visualized the results with Chimera X. The subcellular localization of AcBAMs was predicted by WoLF PSORT (https://www.genscript.com/wolf-psort.html) and further confirmed by CELLO [28].

Sequence alignment, phylogenetic, and collinearity analysis of AcBAMs

The protein sequences of AcBAMs were aligned by using the ClustalW (v1.0) software and showed by the DNAMAN (v5.0). The resultant alignment was used to compute the phylogenetic tree through the maximum-likelihood method with 1000 bootstrap replicates using MEGA X (v11.0.1) [29]. To get the phylogenetic tree between different species, the BAM genes' amino sequences of Arabidopsis (TAIR v10.1), rice (AGIS v1.0), tomato (SLM_r2.1), citrus (Citrus sinensis v3.0), and apple (GDT2T_hap1) were obtained from TAIR (http://www.arabidopsis.org), TIGR rice databases (http://www.tigr.org/tdb/e2k1/osa1), Sol Genomics Network (https://solgenomics.net/), Citrus Pan-genome to Breeding Database (http://citrus.hzau.edu.cn/) and the apple genome database (http://genomics.research.iasma.it/), respectively. A total of 88 BAM genes were further constructed in the phylogenetic in the same method as before. Then used the ITOL (https://itol.embl.de/) to visualize the tree. Intraspecific collinearity analysis was conducted using the 'MCScanX' plug-in within TBtools, utilizing the kiwifruit genome, GFF3 files, and amino acid sequences of AcBAMs [30].

Motif analysis, intron/exon distribution, and cis-element prediction of AcBAMs

MEME (https://meme-suite.org/meme/) was employed to identify conserved motifs, with a maximum number of motifs of 10 with default parameters. Gene structure information was extracted from the 'Hongyang'genome annotation file by using TBtools (v2.119). Cis-elements in the promoter region of *AcBAMs* were predicted by Plantcare [31]. All results were visualized by using TBtools [30].

Expression profiling of AcBAMs

The extraction of total RNA from plants uses a kit (Aidlab, RN33, China) [32]. Refer to the instructions for specific operation methods. The purity and concentration of

RNA were detected by a nanodrop 2000 spectrophotometer (Thermo Fisher Scientific, Waltham, MA, USA). The cDNA libraries construction and the high throughput transcriptome sequencing were performed by BioMarker Technology Co., Ltd (Shanghai, China) using a Qseq400 System (Invision, Shanghai, China). After sequencing, the raw reads were filtered, and clean data were obtained by removing low-quality reads and adapter sequences. High-quality clean data were aligned to the reference genome sequence of kiwifruit with HISAT2 v. 2.0.1 (http://daehwankimlab.github.io/hisat2/download/). The transcript abundance of *AcBAMs* was calculated as fragments per kilobase of exon model per million mapped reads (FPKM) [33].

The RNA used in qPCR comes from RNA extracted during RNA sequencing. The cDNA was synthesized using a one-step kit (Vazyme, R423-01, China), and the quality and concentration of the synthesized cDNA were determined using nanodrop 2000 spectrophotometer Quantitative real-time PCR (qPCR) was conducted utilizing the ChemQ SYBR Master Mix (Vazyme, Q311-02, China) on an ABI7500 system (Applied Biosystems, Foster City, USA). The amplification protocol involved an initial denaturation at 95 °C for 5 min, followed by 40 cycles of denaturation at 95 °C for 10 s, annealing at 58 °C for 30 s, and extension at 95 °C for 15 s. Reactions were carried out in a total volume of 20 μL, consisting of 10 μL of 2 × SYBR PCR Master Mix, 0.8 μL of primers, and 200 ng of cDNA. Three technical replicates were performed for each sample. Actin served as the internal control to normalize gene expression data, with relative expression levels calculated using the $2(-\Delta\Delta CT)$ method. The primers used in the qPCR were shown in Table S1.

VIGs of AcBAMs in kiwifruit

A specific primer was designed to amplify the nonconservative region of the CDS of 402 BP (*AcBAM5*) and 414 BP (*AcBAM13*). Trelief Sosoo cloning Kit (Qingke, China) was inserted into the pTRV2 vector between BamH I site and SMA I site by the one-step method. The constructed vector was sequenced and transferred into GV3101 competent cells. Agrobacterium tumefaciens containing pTRV1 and pTRV2 were inoculated into LB liquid medium, and cultured for 24–48 h. After 4000 r/min centrifugation, the bacteria were collected and suspended in MES buffer, then pTRV1 and pTRV2 were mixed in a ratio of 1:1. When infecting kiwifruit, gently scraped the back of kiwifruit leaves with a syringe needle, injected Agrobacterium into the leaves from the wound, and cultivated plants at room temperature for 15 days; the control plants were injected with Agrobacterium carrying the empty pTRV2 vector and the pTRV1 vector [34]. Each treatment involved injecting the leaves of three kiwifruit seedlings as biological replicates. Afterward, the injected leaves were collected, quickly frozen in liquid nitrogen, and stored at -80 °C for further analysis. The starch content was determined using kits for starch (Solarbio, BC0700, China) according to the manufacturer's instructions.

Statistical analysis

All experiment data were presented means ± standard deviation (SD). Statistical analysis was performed via one-way ANOVA. Significant differences were evaluated by Duncan's tests using SPSS 17.0 software (SPSS Inc., Chicago, USA), which are indicated by '*' or lowercase ($P < 0.05$). '**' represent $P < 0.01$.

Result

Identification of AcBAM gene family in 'Hongyang' genome

The new version of the complete 'Hongyang' genome (V3.0) including genome sequences, coding sequences, and protein sequences was downloaded from Kiwifruit Genome Database (https://kiwifruitgenome.org/). Then used the conserved domain PF01373 to identify the candidate *BAM* genes in kiwifruit by performing a hidden Markov model (HMM) search, only sequences with E-values smaller than $1e^{-5}$ were retained. SMART, Pfam search and NCBI CD-search were used to ensure the candidate *BAM* genes contain the β-amylase domain. After the above steps, a total of 17 *BAM* genes were identified in the kiwifruit genome, which is larger than the amount of *BAM* genes in other species such as *Arabidopsis*, rice, and apple. These genes were named *AcBAM1* to *AcBAM17* respectively according to their E-value (Table 1).

The molecular properties of AcBAMs were calculated by the Batch Protein Parameters Calc (https://www.uniprot.org). According to the analysis results, the molecular weight of AcBAMs was between 34.0–78.4 kDa, and the isoelectric point was between 5.65–8.93; all AcBAMs were hydrophobic (GRAVY < 0); the structure of AcBAM3-4, AcBAM11 and AcBAM14-16 were unstable (Instability index > 40); eight AcBAMs were located at chloroplast and four AcBAMs were located at Cytoplasm based on the subcellular localization prediction (Table 1).

SOPMA contained several independent algorithms and was used to predict the secondary structure of AcBAMs to enhance the accuracy of calculation results. The content of four secondary structures in AcBAMs was ranked as random coil > α-helix > extended strand (β-sheet) > β-turn except AcBAM14 and AcBAM17, and the proportions of secondary structure in most AcBAMs were almost the same (Fig. S1). Tertiary structure predictions of AcBAMs were also performed by constructing SWISS-PROT models. The GMQE values of AcBAMs

Table 1 Characteristics of AcBAM proteins

Gene ID	Gene Name	Chr.	Protain (aa)	Start Codon	End Codon	Physicochemical Properties				Secondary Structure (%)			
						Molecular Weight	Instability Index	Isoelectric Point (pI)	GRAVY	α-helix	Extended strand	β-turn	Random coil
Actinidia03409.t1	*AcBAM1*	chr.14	547	7641467	7644862	61.83	39.35	8.68	-0.55	34.19	14.08	5.48	46.25
Actinidia25927.t2	*AcBAM2*	chr.24	547	1921467	1952509	61.94	38.62	8.93	-0.56	33.89	14.26	5.56	46.3
Actinidia35931.t1	*AcBAM3*	chr.01	531	16047666	16051276	59.05	43.98	6.14	-0.42	37.85	13.37	6.59	42.18
Actinidia31484.t1	*AcBAM4*	chr.15	497	12956093	12958956	55.79	44.85	8.54	-0.47	33	14.49	6.64	45.88
Actinidia10870.t1	*AcBAM5*	chr.14	394	4204738	4207034	44.35	36.26	8.00	-0.55	35.03	15.74	8.12	41.12
Actinidia20910.t2	*AcBAM6*	chr.18	551	9865330	9872975	62.55	37.10	5.53	-0.39	31.94	12.89	5.81	49.36
Actinidia25096.t2	*AcBAM7*	chr.08	421	16983928	16989354	46.60	38.23	6.77	-0.43	34.68	13.06	5.46	46.79
Actinidia10015.t1	*AcBAM8*	chr.08	697	9875867	9888277	77.84	35.05	5.60	-0.43	33	13.2	6.31	47.49
Actinidia20911.t1	*AcBAM9*	chr.18	700	9875407	9883823	78.41	38.10	5.24	-0.44	31.71	13.14	5.57	49.57
Actinidia30504.t1	*AcBAM10*	chr.13	535	15646828	15651821	60.18	35.25	5.33	-0.40	38.69	12.52	5.79	42.99
Actinidia05008.t2	*AcBAM11*	chr.17	523	11751238	11759501	59.86	48.52	8.83	-0.30	35.18	16.06	7.07	41.68
Actinidia01235.t1	*AcBAM12*	chr.20	644	3975306	3985910	72.66	39.45	6.05	-0.45	35.25	11.96	6.21	46.58
Actinidia00051.t1	*AcBAM13*	chr.29	532	15822310	15825934	58.86	30.30	6.55	-0.28	35.71	12.97	4.89	46.43
Actinidia27300.t1	*AcBAM14*	chr.25	414	6418519	6424045	45.27	41.87	7.52	-0.12	41.6	12.32	6.28	40.34
Actinidia30407.t1	*AcBAM15*	chr.16	370	18069947	18075472	42.01	41.25	5.81	-0.29	36.76	13.51	5.95	43.78
Actinidia30334.t1	*AcBAM16*	chr.25	449	7444729	7452581	49.68	43.86	5.87	-0.42	33.63	12.03	6.9	47.44
Actinidia14163.t1	*AcBAM17*	chr.06	301	42556	43847	34.09	38.17	5.66	-0.14	38.87	15.28	8.31	37.54

were higher than 0.75 which meant all models were highly reliable. Different color represents the position of peptide chains, shows AcBAMs have similar tertiary structures and may have the same biological function (Fig. S1).

The multiple sequence alignment, cluster analysis, gene structure, and motif analysis of AcBAMs

The *AcBAM* family consists of 17 genes. For ease of presentation, we selected 10 genes that have conserved domains and have not undergone mutations in the active site of Glu186 for multiple sequence alignment. The multiple sequence alignment showed that the CDS length of *AcBAMs* ranged from 921 to 2138 bp, and all *AcBAMs* had a β-amylase domain, and the active site of this domain was conserved in these genes (Fig. 1). The cluster analysis divided 17 *AcBAMs* into 3 groups, the result was shown by the phylogenetic tree (Fig. 2a). *AcBAM15*, *AcBAM11*, *AcBAM13*, *AcBAM17* and *AcBAM14* were clustered into Group I; *AcBAM10*, *AcBAM16*, *AcBAM12*, *AcBAM6*, *AcBAM9* and *AcBAM8* were clustered into Group II, *AcBAM7*, *AcBAM3*, *AcBAM5*, *AcBAM4*, *AcBAM2* and *AcBAM1* were clustered into Group III. A total of 10 motifs were identified by performing a MEME search. Motif 4 and motif 5 appeared in all genes, and these amino acid residues were located in the active center of the Glyco_hydro_14 conserved domain in multiple sequence alignment; Other motifs are also conserved in most *AcBAMs*. The NCBI CDD-Search results also showed that all AcBAM proteins had PLN02803 conserved domain, which encoded a β-amylase (Fig. 2b). It is worth noting that although *AcBAM17* has the shortest length, only 307 amino acids, it has a complete β-amylase domain and contains multiple motifs including the active center of PLN02803, so it is considered that *AcBAM17* also belongs to β-amylase family.

To get further insights into the evolution of the β-amylase family in kiwifruit, we analyzed the gene structure of *AcBAMs*. *AcBAM1-5* and *AcBAM7* belonged to group III, and their gene length was shorter, neither exceeding 4000 bp, with 4–5 exons per gene; The length of six genes in group II was much longer than that in group III, and these genes contained 8–10 exons; In group I, *AcBAM11*, *AcBAM15* and *AcBAM17* had 8–10 exons, while *AcBAM13* and *AcBAM14* only had 3 and 4 exons, respectively (Fig. 2c). The result shows genes within the same group exhibited more similar gene structures.

Multi-species phylogenetic analysis of BAM genes

Phylogenetic analysis plays a vital role in understanding the evolutionary relationships of genes among different

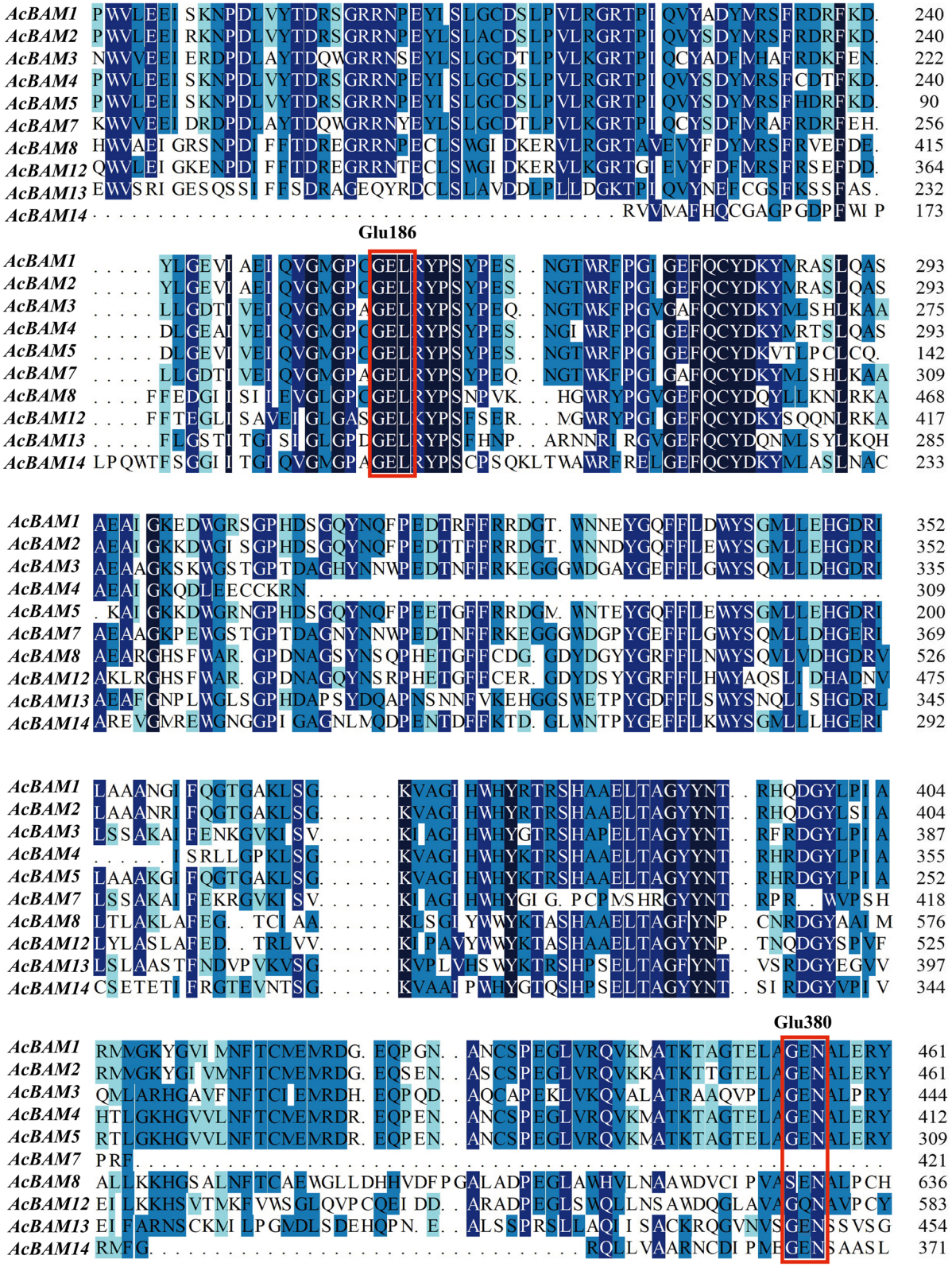

Fig. 1 Multiple sequence alignment of the AcBAM proteins. deep color shading indicates highly conservative substitutions. Red box represents the two catalytic sites Glu-186 and Glu-380

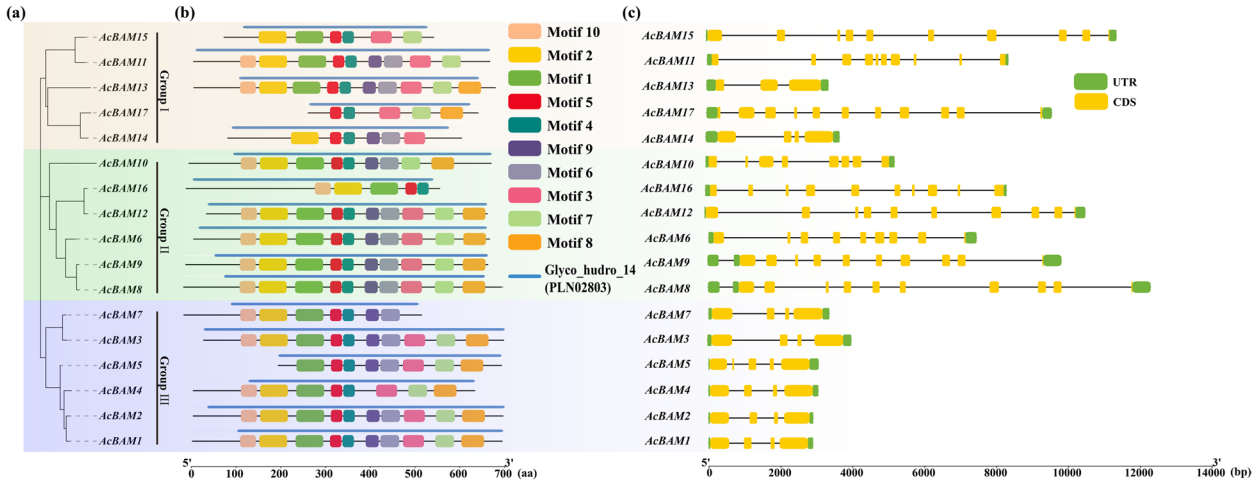

Fig. 2 Bioinformatics analyzes of *AcBAM* genes family. **a** Phylogenetic analysis of *AcBAMs* in kiwifruit. **b** Conserved domain and conserved motif analysis of the *AcBAMs* family. **c** Gene structure analysis of *AcBAMs* family

species. To gain insights into the evolutionary processes of *AcBAMs*, the phylogenetic tree of *BAM* genes in six species including Kiwifruit was constructed by MEGA X. A total of 88 *BAM* genes from different species were clustered into 3 groups. Group 1, group 2, and group 3 contain 14, 28, and 46 genes respectively, and Group 3 was further divided into three subgroups. The clustering results of *BAM* genes among different species were basically consistent with those in kiwifruit, except that *AcBAM17* and *AcBAM14* were clustered into group 2 (Fig. 3). The genetic distance of *AcBAM1*, *AcBAM2*, *AcBAM4* and *AcBAM5* was less than 0.1, and these genes can be clustered with Os10g0565200 (*OsBAM3*), showing that these genes have similar evolutionary paths and biological functions. Both kiwifruit and tomato belong to burries, the phylogenetic tree showed that *AcBAM8* and *AcBAM9* in group 3A could be clustered with seven *BAM* genes from tomato and *AcBAM12* and *AcBAM16* in group 3B could be clustered with other six tomato *BAM* genes, indicating that the protein sequence of these genes may perform similar biological functions and conserved in tomato and kiwifruit. Other *AcBAMs* were also clustered with *BAM* genes from different species (Fig. 3).

Cis-element prediction of AcBAMs promoter

A 1500 bp promoter sequence upstream of *AcBAMs* was used to analyze the cis-elements based on the PlantCARE database. As the result shows, a total of 1175 cis-elements can be divided into four categories: Core cis-element, hormone responsiveness related cis-elements, biotic/abiotic stress responsiveness related cis-elements, plant growth and developmental related cis-elements (Fig. 4). The core cis-elements including CAAT-Box, TATA-Box, and AT ~ TATA-Box, were widely distributed in the promoter region of *AcBAMs*. ABRE was a classic cis-element related to ABA responsiveness and was found in the promoter region of *AcBAM1-10* and *AcBAM13*. It is worth noting that the promoter region of *AcBAM3* and *AcBAM7* contain 16 and 13 ABRE elements respectively (Table S2), indicating that these two genes may be significantly induced by ABA signal. Other hormone responsiveness-related elements were rare in the promoter region of *AcBAMs*. As for biotic/abiotic stress, all *AcBAMs* except *AcBAM5/14* contained DRE, W-Box, or LTR elements related to low-temperature responsiveness (Fig. 4). Other elements related to stress responsiveness such as drought-induced TF binding site MBS were also found in the promoter region of *AcBAMs*. The growth and development related cis-elements including I-Box, G-Box, TCCC-Motif, TCT-Motif, GATA-Motif, and AE-Motif contained in 17 *AcBAMs* promoter regions are basically related to light responsiveness, indicating that the expression of *AcBAMs* may be affected by circadian rhythm.

Intragenomic and intergenomic collinearity analysis of AcBAMs

MCScan X was used to perform the intragenomic and intergenomic collinearity analysis to understand gene duplication events, genome evolution, and the functional implications of genomic rearrangements. As the result shows, 10283 collinear gene pairs were identified in the intrachromosomal and interchromosomal regions, 6 of which were related to the *AcBAM* family (Fig. 5a). Two pairs of genes, *AcBAM6* and *AcBAM9*, *AcBAM14* and *AcBAM16*, were defined as tandem duplication events. Both segmental duplication events and tandem duplication events related to *AcBAMs* can be found in the

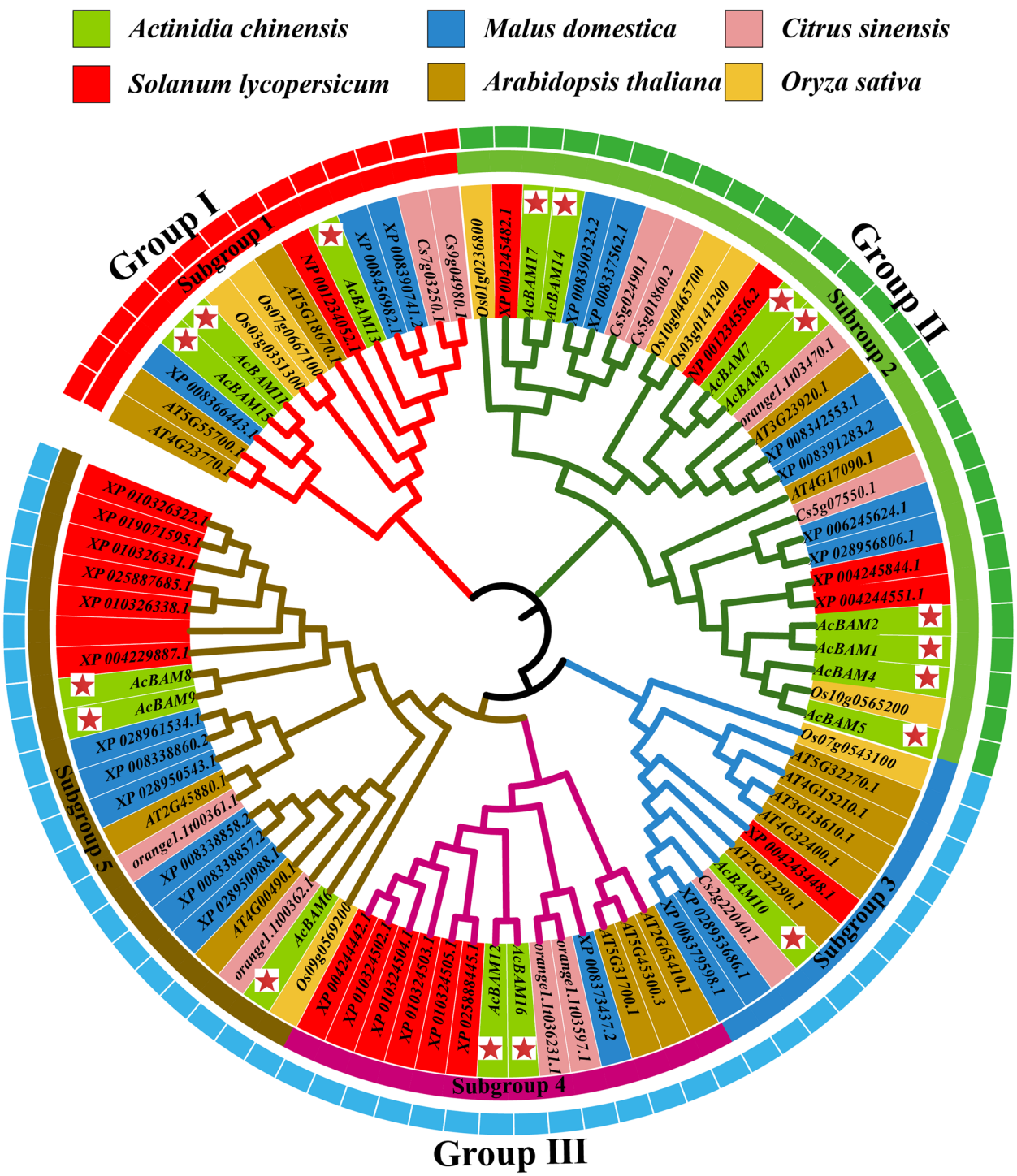

Fig. 3 Phylogenetic analysis of AcBAMs proteins from kiwifruit (*Actinidia chinensis*), *Arabidopsis thaliana*, tomato (*Solanum lycopersicum*), apple (*Malus domestica*), rice (*Oryza sativa*), and citurs (*Citrus sinensis*)

kiwifruit genome, indicating that both two duplication forms contributed to the expansion and evolution of *the AcBAM* family.

The intergenomic collinearity analysis was performed to investigate the evolutionary mechanisms between kiwifruit and the other 5 species. 10, 13, 11, 10, and 4 *AcBAMs* showed collinearity to *BAM* genes from

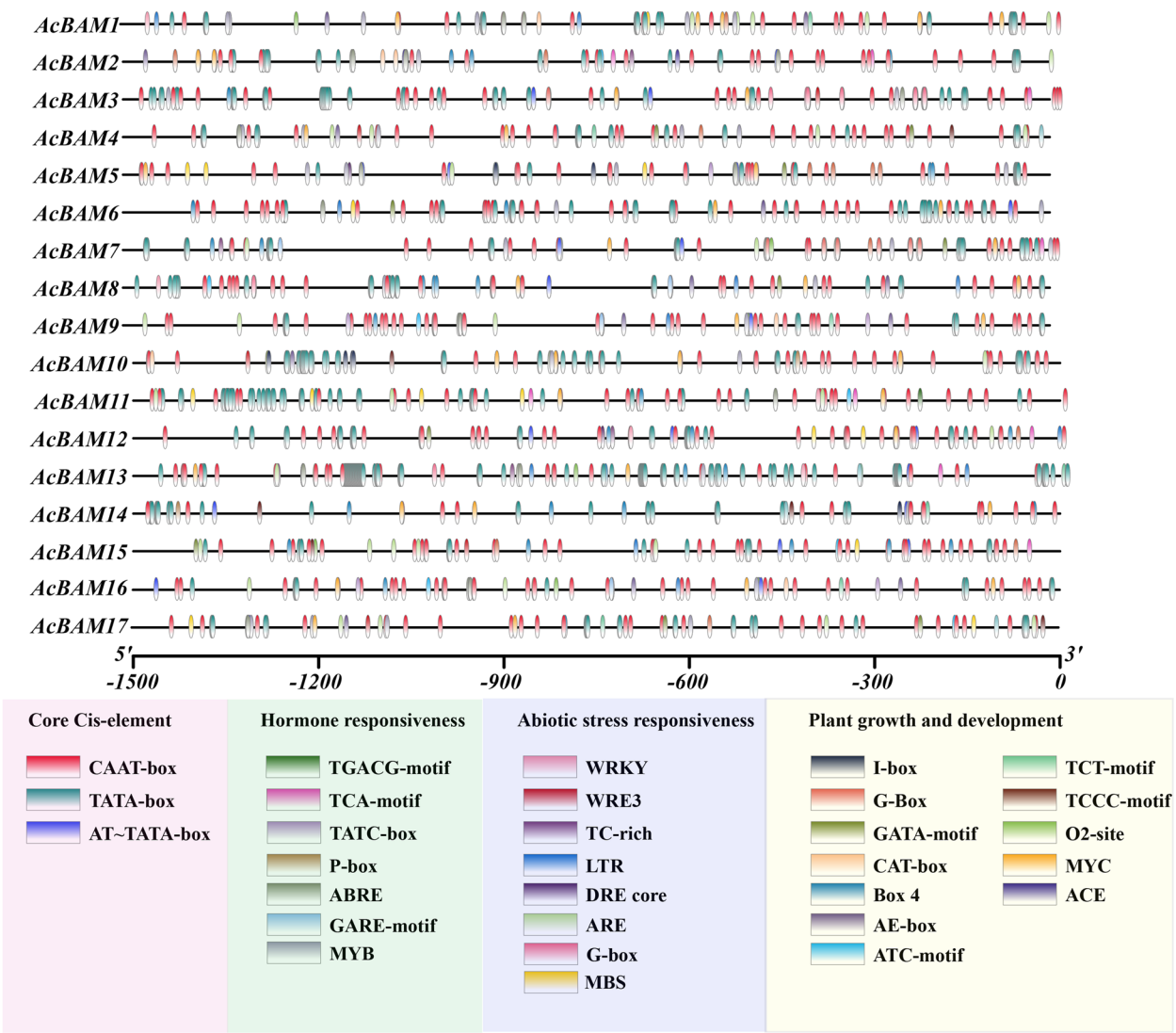

Fig. 4 Cis-elements analysis of the promoter region of *AcBAMs*

Arabidopsis, apple, citrus, tomato, and rice respectively. The collinearity between *AcBAMs* and *BAM* genes in other species reflects their phylogenetic relationship. Twenty-one colinear gene pairs between kiwifruit and apple were identified which is the most amount compared to other species, followed by colinear gene pairs between Arabidopsis and between citrus with 12 pairs each, colinear gene pairs between tomato with 10 pairs, and colinear gene pairs between rice with the least, with only 5 pairs, indicate that the homology of *BAM* genes between kiwifruit and apple is closer, while that between kiwifruit and rice is much further (Fig. 5b). *AcBAMs* of colinear gene pairs were mostly located at chr.25, which is also the location of *AcBAM14* and *AcBAM16*, suggesting that these two genes played an important role in the evolution of *BAM* family in kiwifruit.

The expression patterns of AcBAMs during the post-harvest stage and the expression level of AcBAMs after ABA treatment

To further investigate the expression profile of *AcBAMs* during the storage of 'Hongyang' kiwifruit, we analyzed the RNA-seq database from our laboratory. The FPKM value is used to measure the expression level of *AcBAM*. We also labeled genes in the figure where the FPKM values were greater than 10 and the maximum absolute value of Log2FC between different samples of the same gene exceeded 0.5, to provide a more intuitive comparison of gene expression differences between

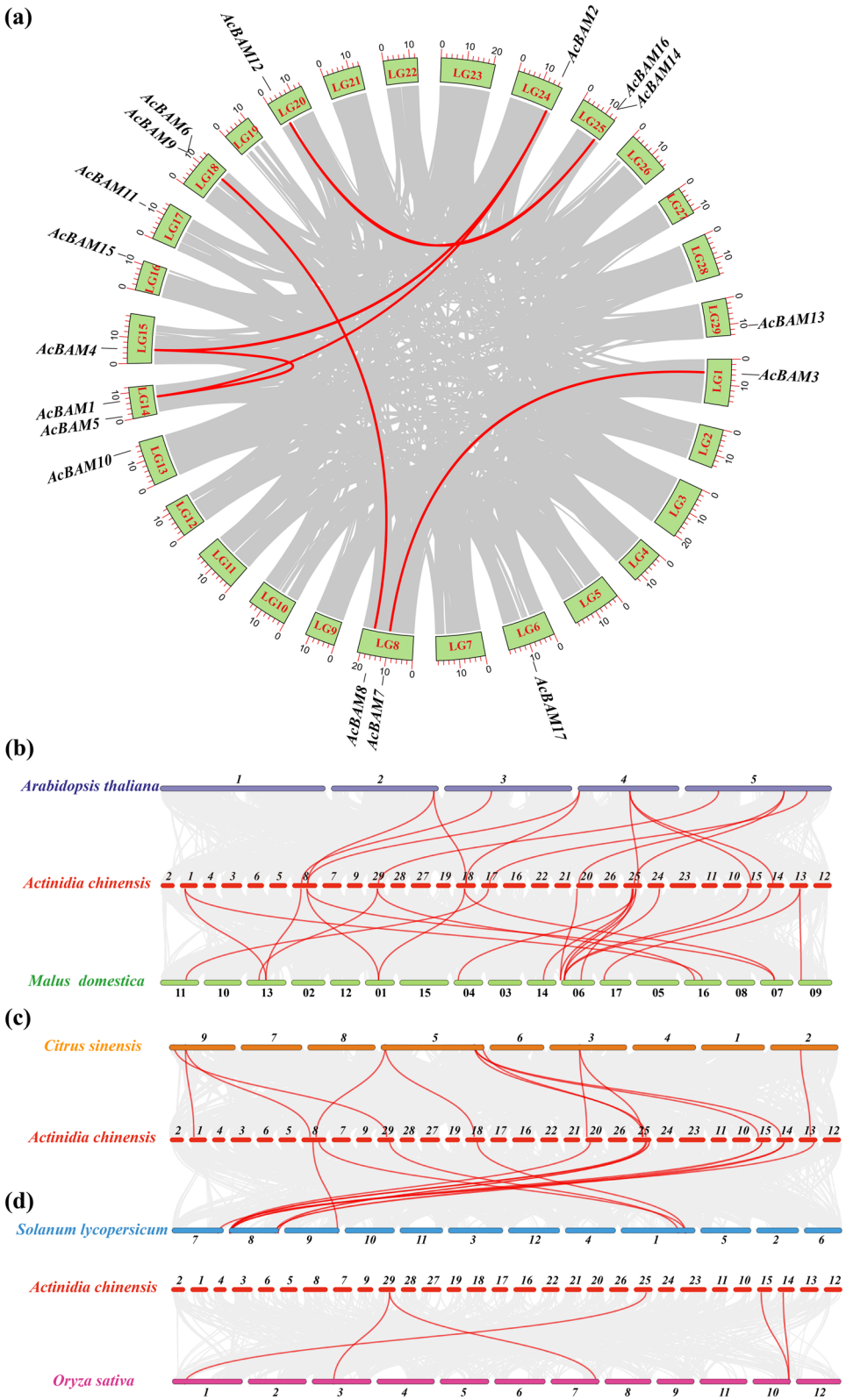

Fig. 5 Collinearity analysis of *AcBAMs*, red lines indicate the collinear relationship between the two *BAM* genes connected. **a** Intergenomic collinearity analysis of kiwifruit. **b**, **c**, **d** Intragenomic collinearity analysis of *AcBAMs* among kiwifruit (*Actinidia chinensis*), *Arabidopsis thaliana*, tomato (*Solanum lycopersicum*), apple (*Malus domestica*), rice (*Oryza sativa*), and citrus (*Citrus sinensis*)

samples. All genes' expression can be detected during storage except *AcBAM10* (Fig. 6a). The expression of *AcBAM1*, *AcBAM4*, *AcBAM5*, *AcBAM13*, and *AcBAM17* increased gradually during kiwifruit postharvest storage, reached the highest level at 8–12 days after harvest. The FPKM values of *AcBAM5* and *AcBAM13* were 4337 and 2786 respectively on the 8th day after harvest, which was much higher than other *AcBAMs* at this period. To further confirm the accuracy of the transcriptome data, we also conducted qPCR experiments. The results were generally consistent with the transcriptome data, showing that the expression levels of *AcBAM5* and *AcBAM13* increased during fruit storage; and after 12 days of storage, their expression levels were significantly higher than those of other genes (Fig. 6b) The expression of another two genes, *AcBAM3* and *AcBAM7*, were different from *AcBAM1*, *AcBAM4*, *AcBAM5*, *AcBAM13*, and *AcBAM17*. The expression levels of the rest nine *AcBAMs* during storage were much lower than those of the seven genes mentioned before (FPKM < 10), which may not be related to the starch degradation process of kiwifruit after harvest.

As the result of promoter sequence analysis shows, ABRE was the most frequent motif related to hormone responsiveness in *the AcBAMs* promoter region and could be found in the promoter of *AcBAM1-10* and *AcBAM13* (Fig. 4). To ensure whether the ABA signal could influence the expression of *AcBAMs* during the post-harvest stage, we analyzed the RNAseq data of kiwifruit after ABA treatment, and four genes (*AcBAM1*, *AcBAM4*, *AcBAM5* and *AcBAM13*) were found to be upregulated. The difference in FPKM values of *AcBAM1*, *AcBAM4*, and *AcBAM5* increased 9 h after treatment and reached the peak at 72 h after treatment, indicating that ABA affected these three genes' expression very quickly and this influence would last for a comparatively long time (Fig. 6c). The expression level of *AcBAM13* showed significant difference at 18 h after treatment, which was slower than *AcBAM1*, *AcBAM4* and *AcBAM5*. Moreover, *AcBAM5* and *AcBAM13* are strongly induced by ABA signaling, with their expression levels significantly higher than all other genes after 36 h of treatment; Other *AcBAMs* were not induced by ABA treatment, and their expression level was much lower compared to *AcBAM1*, *AcBAM4*, *AcBAM5*, and *AcBAM13*(Fig. 6d).

The RNAseq database of low-temperature treated kiwifruit was also analyzed to ensure *AcBAMs* were induced by low-temperature treatment. It was evident that the expression of *AcBAM1*, *AcBAM2*, and *AcBAM5* was strongly induced after 5 ℃ storage, and the expression of *AcBAM7* was inhabited by low temperature (Fig. 6e, f). *AcBAM2* seems not to play a role in the postharvest storage in room temperature, but the expression of it was dramatically increased after low-temperature treatment, showing this gene may function in the pathway relying on cold signal(Fig. 6e, f).

TRV-mediated gene silencing of AcBAM5 and AcBAM13

Both *AcBAM5* and *AcBAM13* had the complete glyco_hydro_14 conserved domain, and the expression of these two genes was strongly induced during the fruit storage and after ABA treatment. To further investigate the function of *AcBAM5* and *AcBAM13*, we used the VIGs system to silence them in kiwifruit. The results of RT-qPCR showed that the expression of *AcBAM5* and *AcBAM13* was significantly decreased to different extents, indicating the VIGS system worked (Fig. 7a). In contrast to the expression trend, the starch content in leaves increased significantly after silencing *AcBAM5* and *AcBAM13*, indicating that these two genes play an important role in the degradation of starch in kiwifruit (Fig. 7b).

Discussion

Starch serves as the primary organic component accumulated during kiwifruit development. At harvest time, the starch content in kiwifruit can reach 15%—30% of its fresh weight. The degradation process of starch during postharvest storage is crucial for kiwifruit to develop its unique flavor. β-amylase is the key enzyme related to starch degradation, which can efficiently degrade amylose into single maltose molecules [35]. In this study, a total of 17 *BAM* genes were identified in the genome of 'Hongyang' kiwifruit, which was distributed across 13 chromosomes, a significantly higher number compared to *BAM* genes in Arabidopsis, rice, tomato, apple, and citrus [36–40]. Recent studies have proved that three genome-wide duplication events occurred during kiwifruit evolution, two of which occurred after the Cretaceous—Palaeogene [41, 42]. These events likely contributed to the expansion of kiwifruit chromosomes to 29 pairs, and the number

(See figure on next page.)

Fig. 6 Expression analysis of *AcBAMs*. **a** The expression of *AcBAMs* during the post-harvest storage, different colored blocks representing different levels of FPKM value. **b** qPCR analysis of *AcBAMs* during the post-harvest storage. **c** The expression of *AcBAMs* after ABA treatment, different colored blocks representing different levels of FPKM value. **d** qPCR analysis of of *AcBAMs* after ABA treatment. **e** The expression of *AcBAMs* during low-temperature storage, different colored blocks representing different levels of FPKM value; T5, T15, and T25 represent kiwifruit stored in environments of 5 ℃, 15 ℃, and 25 ℃, respectively. **f** qPCR analysis of of *AcBAMs* during low-temperature storage

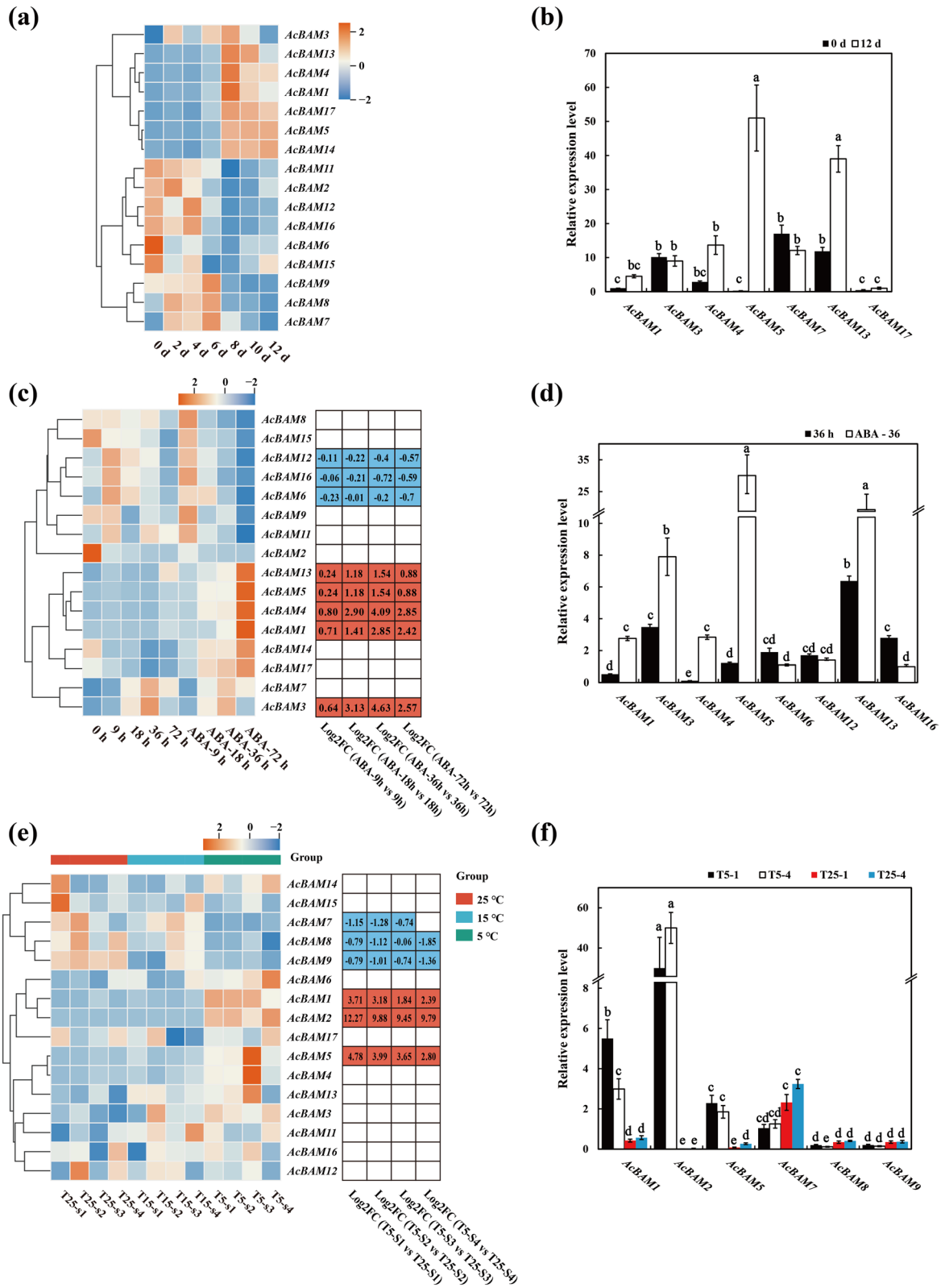

Fig. 6 (See legend on previous page.)

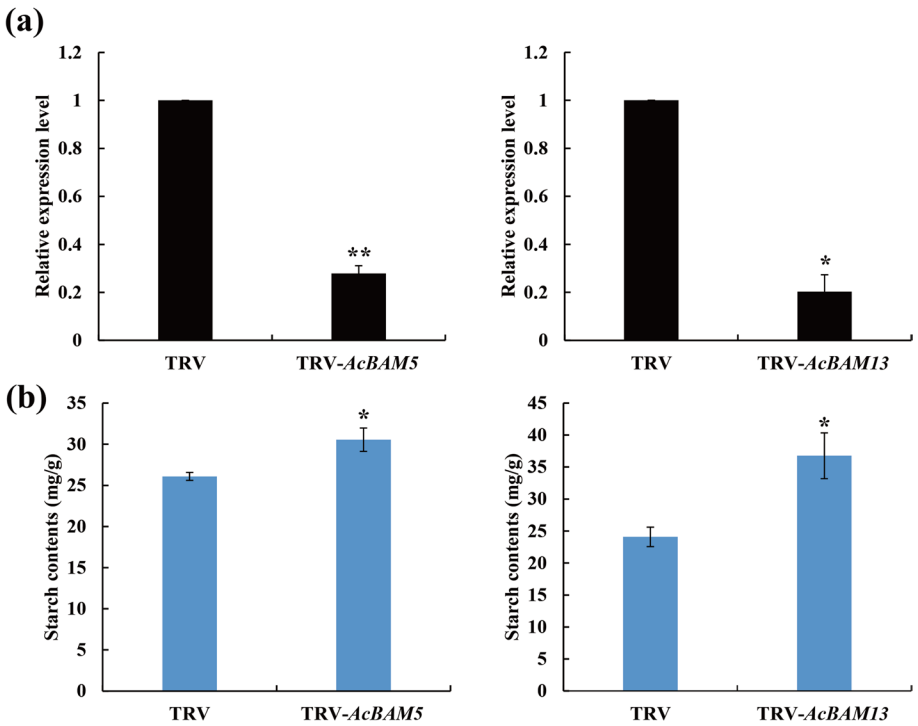

Fig. 7 The TRV-mediated silencing of *AcBAMs*. **a** The expression of *AcBAMs* after treatment. **b** The starch content of kiwifruit leaves after treatment. '*' and '**' represent $P < 0.05$ and $P < 0.01$, respectively

of *BAM* genes increased to 17. In the collinearity analysis, the evidence of WGD events, such as a large number of collinearity between some fragments of chr.13 and chr.23 (Fig. 5A), could also be found easily. Segmental duplication events have been the primary driver for gene expansion in plant genomes. Notably, in the collinearity analysis of jujube, no collinearity was found among *BAM* genes, and only 9 *BAM* genes were found [43]; However, there were a large number of *BAM* collinear gene pairs in upland cotton genome, and the number of *BAM* genes reached 27 correspondingly [44]. That difference in the number of *BAM* genes between jujube and upland cotton is possibly attributed to a segment duplication event. In the kiwifruit genome, six segmental duplication events among 9 *AcBAMs* were observed. Although *AcBAM1*, *AcBAM2*, and *AcBAM4* were located on different chromosomes respectively, the collinearity relationships were still identified between them. The collinearity analysis between kiwifruit and apple genomes shows that both these three genes were collinear with *MaBAM4*, indicating that they had a similar evolution pathway, and it was likely that one of them was expanded to three *BAM* genes due to the chromosome segment replication event, and the replication event should occur later than the differentiation between apple and kiwifruit, which also explains the reason for the increase in the number of *BAM* genes in kiwifruit. Additionally, a pair of tandem repeat genes, *AcBAM14* and *AcBAM16*, located in chr.25, showed collinearity with multiple *BAM* genes in other species, suggesting their significant role in the evolution of *BAM* genes. To gain insight into the evolutionary relationships of genes or species, we constructed a phylogenetic tree of *BAM* genes. Phylogenetic analysis involving *AcBAMs* and *BAM* genes from other species revealed that *AcBAMs* were found to be distributed across all groups, and the genetic distance of *AcBAMs* between different groups was greater, indicating that the replication events had occurred at earlier stages (Fig. 3); *AcBAMs* can be clustered with *BAM* genes in other species, which also shows that these genes may have similar structure and biological functions.

Typical *BAM* genes all have a glyco_hydro_14 conserved domain, which is crucial for the *BAM* gene to perform biological functions [45]. The active center of BAM contains a flexible loop (96-103aa) and an inner loop (340—346aa) [46]. When BAM starts to degrade starch, two molecules of maltose in the starch chain will combine in these two loops respectively. Then Glu186 and Glu380 are used as catalytic residues to catalyze the hydrolysis of starch [47]. In the multiple sequence alignment of AcBAMs, the catalytic site of Glu186 was conserved in all AcBAMs, and the tertiary structure of the

protein was similar; However, Glu380 was deleted or mutated in AcBAM7, AcBAM10, AcBAM11, AcBAM12, AcBAM15, and AcBAM16, with substitutions predominantly from glutamate (E) to glutamine (Q). This pattern mirrors observations in Arabidopsis [48] and rice BAM1 [49], where analogous mutations abolished catalytic activity, suggesting convergent evolution of non-functional BAM paralogs across divergent species.

BAM is a multigene family in plants, but certain *BAM* genes may not function during different development stages or organs in plants. Many plant genomes in nature contain multiple BAM genes. Except for those genes whose biological activity is lost due to mutations in catalytic sites or other reasons, the remaining functional *BAM* genes exhibit spatiotemporal expression specificity, and thus play roles in different tissues or physiological processes [50–52]. For example, Research on tomatoes indicates that *SlBAM2* is predominantly active in leaves, whereas *SlBAM5* is the major contributor to starch accumulation in fruits [39]. To elucidate which genes play a key role in starch degradation during the postharvest ripening process of kiwifruit, we analyzed the expression patterns of the *AcBAM* gene family in kiwifruit after harvest. Through transcriptome sequencing analysis and qPCR analysis of 'Hongyang' kiwifruit at the post-harvest stage, it was found that the expression of *AcBAM5* and *AcBAM13* gradually increased with fruit storage, reaching 4508 and 2786, respectively, which were significantly higher than those of other *BAM* genes. After silencing *AcBAM5* and *AcBAM13* in kiwifruit, the starch content in leaves increased significantly, suggesting that these two genes played an important role in the accumulation of soluble sugar during the post-harvest ripening process of kiwifruit.

Abscisic acid (ABA) is a plant hormone that plays a vital role in various physiological processes within plants. Previous studies were more focused on the regulation of *BAM* genes expression by ABA in response to drought and ion stress in the aboveground parts of plants, and limited studies had discussed the influence of ABA on the degression of starch in postharvest fruits [53]. In our study, we found the presence of ABRE (ABA-responsive elements) that respond to ABA signals in the promoter regions of *AcBAM5*, and *AcBAM13*, and the expression of these four genes were strongly induced by ABA treatment. This suggests that these two genes may not only be involved in the natural starch degradation process during kiwifruit ripening but also play a key role in the ABA-induced starch degradation process (Fig. 6d). Notably, in climacteric fruits like strawberry, exogenous ABA accelerates starch-to-sugar conversion by upregulating amylase genes, suggesting the possibility of utilizing ABA or ABA analogues in postharvest kiwifruit treatments to facilitate rapid ripening [54, 55]. *AcBAM3* and *AcBAM7* also contain multiple ABRE elements in their promoter regions, but their expression is not significantly induced by ABA. It is speculated that the response of *AcBAM3* and *AcBAM7* to ABA is not simply mediated by ABF (ABRE-binding transcription factor), and further investigation is required to unravel the specific molecular mechanisms underlying this phenomenon.

The expression of *BAM* family genes has also been proven to be influenced by abiotic stress. For instance, In arabidopsis, *BAM* genes' expression in leaves can be induced by light and soluble sugars, and participate in the subsequent reaction of plant photosynthesis, but its expression will be inhibited by gibberellic acid (GA) [56]; Similar studies conducted in vitis amurensis and pear also showed that *VaBAM1* and *PtrBAM3* were strongly induced by low temperature, and the cold resistance of plants was improved by degrading starch to improve the cytoplasmic osmotic potential [40, 57]. Upon analyzing the promoter elements of *AcBAMs*, it was observed that the promoter regions of these genes contain numerous low-temperature response elements such as LTR, CRT, and DRE. Transcriptome analysis demonstrated that *AcBAM1*, *AcBAM2*, and *AcBAM5* were genuinely induced by low-temperature treatment, especially the expression of *AcBAM2*, which was up-regulated over 1,000 times, and the Log_2FC of stage-S1 reached 12.27 which meant the expression of *AcBAM2* showed significantly different compared to room temperature treatment. Generally, it is believed that the low-temperature storage of fruit leads to a reduction in the activities of various enzymes in the fruit and prolongs the storage period [58, 59]. However, recent studies in kiwifruit have revealed that a low-temperature environment ranging from 5—10 °C can promote the ripening process of kiwifruit, leading to an increase in soluble solids content and a decrease in organic acids, and this responsiveness to cold signal did not depend on the participation of ethylene [60]. *AcBAM1*, *AcBAM2*, and *AcBAM5* are also involved in the ripening process of kiwifruit under low-temperature storage in this manner.

Conclusion

In conclusion, our study identified 17 *BAM* genes in the genome of 'Hongyang' kiwifruit, which is significantly higher compared to other plant species. Multiple duplication and segmental duplication events contributed to the expansion of the *BAM* gene family in kiwifruit. The conserved glyco_hydro_14 domain and catalytic residues in BAM proteins indicated that not all *AcBAMs* have catalytic activity. Phylogenetic analysis revealed the evolutionary relationships among *BAM* genes in

different species, highlighting their structural and functional similarities. Transcriptome analysis identified *AcBAM5* and *AcBAM13* as highly expressed during kiwifruit ripening. Silencing *AcBAM5* and *AcBAM13* resulted in a significant increase in starch content in leaves, indicating their roles in soluble sugar accumulation. Additionally, the expression of *BAM* genes in kiwifruit was influenced by abiotic factors, such as low temperature and ABA treatment. Our study provides insights into the regulation of the *BAM* gene family in postharvest kiwifruit, advancing the understanding of starch degradation and fruit ripening processes.

Abbreviations

BAM	β-Amylase
T/A	Total soluble solids to total acidity
MW	Molecular weight
GRAVY	Grand average hydropathicity
pI	Theoretical isoelectric point
CDD	Conserved domain
CDS	Coding sequence
Glyco_hydro_14	Glycoside hydrolase 14 super family
ABRE	Abscisic acid responsive element
FPKM	Fragments per kilobase of exon model per million mapped fragment
RT-qPCR	Quantitative real-time polymerase chain reaction
WGD	Whole genome duplicate event
ABF	ABRE-binding transcription factor
GA	Gibberellic acid
ABA	Abscisic acid

Supplementary Information

The online version contains supplementary material available at https://doi.org/10.1186/s12870-025-06425-w.

Supplementary Material 1: Figure S1: Senior structure analysis of AcBAMs. a) Three-dimensional diagram of AcBAMs protein tertiary structure. B) Protein secondary structure analysis of AcBAMs.

Supplementary Material 2: Figure S2: Rectangular Phylogenetic Tree of the AcBAM Gene Family between kiwifruit (*Actinidia chinensis*), *Arabidopsis thaliana*, tomato (*Solanum lycopersicum*), apple *(Malus domestica*), rice (*Oryza sativa*), and citrus (*Citrus sinensis*).

Supplementary Material 3: Table S1. Primers used in this study.

Supplementary Material 4: Table S2. *Cis*-acting elements in the promoter region of *AcBAMs*.

Acknowledgements
Not applicable.

Authors' contributions
XG: Writing – review & editing, Writing – original draft, Methodology, Data curation; bioinformatic analysis. ML: qRT-PCR experiment; experimental treatmental. JS and DY: Language polishing; VIGs experiment carrying out. ZG and XW: Experimental guidance and paper revision. All authors reviewed the manuscript.

Funding
This research was supported by the Basic Research and Talent Program of Jiangxi Academy of Sciences (2022YRCG001; 2022YRCS003; 2022YYB21), the Open Funds of The National Key Laboratory for Germplasm Innovation & Utilization of Horticultural Crops (Horti-KF-2023–15) and the Jiangxi Provincial Natural Science Foundation Youth Fund Project (20232BAB215040).

Data availability
The datasets used and/or analysed during the current study are available from the corresponding author on reasonable request. The raw data of RNA-sequencing have been deposited with CNCB (https://download.cncb.ac.cn/gsa/) under BioProject PRJCA035858.

Declarations

Ethics approval and consent to participate
Not applicable.

Consent for publication
Not applicable.

Competing interests
The authors declare no competing interests.

Author details
[1]Jiangxi Provincial Key Laboratory of Plantation and High Valued Utilization of Specialty Fruit Tree and Tea, Institute of Biological Resources, Jiangxi Academy of Sciences, Nanchang, Jiangxi, China. [2]Jiangxi Kiwifruit Engineering Research Center, Nanchang, Jiangxi, China. [3]Jiangxi Agricultural University, Nanchang, Jiangxi, China.

Received: 15 October 2024 Accepted: 19 March 2025
Published online: 02 April 2025

References

1. Ferguson AR, Huang H, Costa G. History of Kiwifruit: Evolution of a Global Crop. Botany, Production and Uses. 2023: 1–15.
2. Liu Q, Li X, Jin S, et al. γ-Aminobutyric acid treatment induced chilling tolerance in postharvest kiwifruit (*Actinidia chinensis* cv. Hongyang) via regulating ascorbic acid metabolism. Food Chem. 2023; 404: 134661.
3. Jin M, Jiao J, Zhao Q, et al. Dose effect of exogenous abscisic acid on controlling lignification of postharvest kiwifruit (Actinidia chinensis cv. hongyang). Food Control. 2021; 124: 107911.
4. Chen Y, Hu X, Shi Q, et al. Changes in the fruit quality, phenolic compounds, and antioxidant potential of red-fleshed kiwifruit during postharvest ripening. Foods. 2023;12(7):1509.
5. Li D, Zhu F. Physicochemical properties of kiwifruit starch. Food Chem. 2017;220:129–36.
6. Mao J, Gao Z, Lin M, et al. Targeted multi-platform metabolome analysis and enzyme activity analysis of kiwifruit during postharvest ripening. Front Plant Sci. 2023;14:1120166.
7. Manolopoulou H, Papadopoulou P. A study of respiratory and physicochemical changes of four kiwi fruit cultivars during cool-storage. Food Chem. 1998;63(4):529–34.
8. Manolopoulou H, Papadopoulou P. Respiratory and compositional changes of kiwifruit cultivars during air atmosphere storage at 0 C. III International Symposium on Kiwifruit. 1995;444:547–54.
9. Hallett IC, Wegrzyn TF, MacRae EA. Starch degradation in kiwifruit: in vivo and in vitro ultrastructural studies. Int J Plant Sci. 1995;156(4):471–80.
10. Silver DM, Kötting O, Moorhead GBG. Phosphoglucan phosphatase function sheds light on starch degradation. Trends Plant Sci. 2014;19(7):471–8.
11. Kötting O, Pusch K, Tiessen A, et al. Identification of a novel enzyme required for starch metabolism in Arabidopsis leaves. The phosphoglucan, water dikinase. Plant Physiol. 2005; 137(1): 242–252.
12. Hejazi M, Fettke J, Paris O, et al. The two plastidial starch-related dikinases sequentially phosphorylate glucosyl residues at the surface of both the A-and B-type allomorphs of crystallized maltodextrins but the mode of action differs. Plant Physiol. 2009;150(2):962–76.
13. Santelia D, Kötting O, Seung D, et al. The phosphoglucan phosphatase like sex Four2 dephosphorylates starch at the C3-position in Arabidopsis. Plant Cell. 2011;23(11):4096–111.
14. Schreier TB, Umhang M, Lee SK, et al. LIKE SEX4 1 acts as a β-amylase-binding scaffold on starch granules during starch degradation. Plant Cell. 2019;31(9):2169–86.

15. Liu J, Wang X, Guan Z, et al. The LIKE SEX FOUR 1–malate dehydrogenase complex functions as a scaffold to recruit β-amylase to promote starch degradation. Plant Cell. 2024;36(1):194–212.
16. Zeeman SC, Kossmann J, Smith AM. Starch: its metabolism, evolution, and biotechnological modification in plants. Annu Rev Plant Biol. 2010;61:209–34.
17. Weise SE, Kim KS, Stewart RP, et al. β-Maltose is the metabolically active anomer of maltose during transitory starch degradation. Plant Physiol. 2005;137(2):756–61.
18. David LC, Lee SK, Bruderer E, et al. BETA-AMYLASE9 is a plastidial nonenzymatic regulator of leaf starch degradation. Plant Physiol. 2022;188(1):191–207.
19. Peroni FHG, Koike C, Louro RP, et al. Mango starch degradation. II. The binding of α-amylase and β-amylase to the starch granule. J Agric Food Chem. 2008;56(16):7416–21.
20. Miao H, Sun P, Miao Y, et al. Genome-wide identification and expression analysis of the β-amylase genes strongly associated with fruit development, ripening, and abiotic stress response in two banana cultivars. Front Agric Sci Eng. 2017;3(4):346–56.
21. Li M, Chen X, Huang W, et al. Comprehensive Identification of the β-Amylase (BAM) Gene Family in Response to Cold Stress in White Clover. Plants. 2024;13(2):154.
22. Li YQ, Gao H, Jia DF, et al. AGPS and BAM genes dramatically improve 'Ganlv 1'(Actinidia eriantha) fruit quality through starch metabolism during fruit development. Sci Hortic. 2024;329: 113004.
23. Hu X, Kuang S, Zhang AD, et al. Characterization of starch degradation related genes in postharvest kiwifruit. Int J Mol Sci. 2016;17(12):2112.
24. Wu H, Ma T, Kang M, et al. A high-quality *Actinidia chinensis* (kiwifruit) genome. Horticulture Research. 2019;6:117.
25. Chen C, Chen X, Han J, et al. Genome-wide analysis of the WRKY gene family in the cucumber genome and transcriptome-wide identification of WRKY transcription factors that respond to biotic and abiotic stresses. BMC Plant Biol. 2020;20:1–19.
26. Zhang Z, Chen J, Liang C, et al. Genome-wide identification and characterization of the bHLH transcription factor family in pepper (Capsicum annuum L.). Front Genet. 2020;11:570156.
27. Li P, Chai Z, Lin P, et al. Genome-wide identification and expression analysis of AP2/ERF transcription factors in sugarcane (Saccharum spontaneum L.). BMC genomics. 2020;21:1–17.
28. Yang J, Zhang B, Gu G, et al. Genome-wide identification and expression analysis of the R2R3-MYB gene family in tobacco (Nicotiana tabacum L.). BMC genomics. 2022;23(1):432.
29. Liu F, Li H, Wu J, et al. Genome-wide identification and expression pattern analysis of lipoxygenase gene family in banana. Sci Rep. 2021;11(1):9948.
30. Chen C, Wu Y, Li J, et al. TBtools-II: A "one for all, all for one" bioinformatics platform for biological big-data mining. Mol Plant. 2023;16(11):1733–42.
31. Hoffmann TD, Kurze E, Liao J, et al. Genome-wide identification of UDP-glycosyltransferases in the tea plant (Camellia sinensis) and their biochemical and physiological functions. Front Plant Sci. 2023;14:1191625.
32. Song J, Sun P, Kong W, et al. SnRK2.4 - mediated phosphorylation of ABF2 regulates ARGININE DECARBOXYLASE expression and putrescine accumulation under drought stress. New Phytol. 2023; 238(1): 216–236.
33. Zhao Y, Li MC, Konaté MM, et al. TPM, FPKM, or normalized counts? A comparative study of quantification measures for the analysis of RNA-seq data from the NCI patient-derived models repository. J Transl Med. 2021;19(1):269.
34. Song J, Sun P, Kong W, et al. SnRK2. 4-mediated phosphorylation of ABF2 regulates ARGININE DECARBOXYLASE expression and putrescine accumulation under drought stress. New Phytologist, 2023, 238(1): 216–236.
35. Kang YN, Tanabe A, Adachi M, et al. Structural analysis of threonine 342 mutants of soybean β-amylase: role of a conformational change of the inner loop in the catalytic mechanism. Biochemistry. 2005;44(13):5106–16.
36. Monroe JD, Storm AR. The Arabidopsis β-amylase (BAM) gene family: diversity of form and function. Plant Sci. 2018;276:163–70.
37. Zhang D, Wang Y. β-amylase in developing apple fruits: activities, amounts, and subcellular localization. Life Sci. 2002;45:429–40.
38. Wang SM, Lue WL, Eimert K, et al. Phytohormone-regulated β-amylase gene expression in rice. Plant Mol Biol. 1996;31:975–82.
39. Fan X, Lin H, Ding F, et al. Jasmonates Promote β-Amylase-Mediated Starch Degradation to Confer Cold Tolerance in Tomato Plants. Plants. 2024;13(8):1055.
40. Peng T, Zhu X, Duan N, et al. PtrBAM1, a β-amylase-coding gene of P oncirus trifoliata, is a CBF regulon member with function in cold tolerance by modulating soluble sugar levels. Plant Cell Environ. 2014;37(12):2754–67.
41. Yao X, Wang S, Wang Z, et al. The genome sequencing and comparative analysis of a wild kiwifruit Actinidia eriantha. Mol Hortic. 2022;2(1):13.
42. Wu H, Ma T, Kang M, et al. A high-quality Actinidia chinensis (kiwifruit) genome. Hortic Res. 2019;6(2):13–9.
43. Ma Y, Han Y, Feng X, et al. Genome-wide identification of BAM (β-amylase) gene family in jujube (Ziziphus jujuba Mill.) and expression in response to abiotic stress. BMC genomics. 2022; 23(1): 438.
44. Yang Y, Sun F, Wang P, et al. Genome-Wide Identification and Preliminary Functional Analysis of BAM (β-Amylase) Gene Family in Upland Cotton. Genes. 2023;14(11):2077.
45. Monroe JD, Breault JS, Pope LE, et al. Arabidopsis β-amylase2 is a K+-requiring, catalytic tetramer with sigmoidal kinetics. Plant Physiol. 2017;175(4):1525–35.
46. Mikami B, Adachi M, Kage T, et al. Structure of raw starch-digesting Bacillus cereus β-amylase complexed with maltose. Biochemistry. 1999;38(22):7050–61.
47. Kang YN, Adachi M, Utsumi S, et al. The roles of Glu186 and Glu380 in the catalytic reaction of soybean β-amylase. J Mol Biol. 2004;339(5):1129–40.
48. Fulton DC, Stettler M, Mettler T, et al. β-AMYLASE4, a noncatalytic protein required for starch breakdown, acts upstream of three active β-amylases in Arabidopsis chloroplasts. Plant Cell. 2008;20(4):1040–58.
49. Yamaguchi J, Itoh S, Saitoh T, et al. Characterization of β-amylase and its deficiency in various rice cultivars[J]. Theor Appl Genet. 1999;98:32–8.
50. Monroe JD, Storm AF, Badley EM, et al. β-Amylase1 and β-amylase3 are plastidic starch hydrolases in Arabidopsis that seem to be adapted for different thermal, pH, and stress conditions. Plant Physiol. 2014;166(4):1748–63.
51. Scheidig A, Fröhlich A, Schulze S, et al. Downregulation of a chloroplast-targeted β-amylase leads to a starch-excess phenotype in leaves. Plant J. 2002;30(5):581–91.
52. Valerio C, Costa A, Marri L, et al. Thioredoxin-regulated β-amylase (BAM1) triggers diurnal starch degradation in guard cells, and in mesophyll cells under osmotic stress. J Exp Bot. 2011;62(2):545–55.
53. Zhang Q, Pritchard J, Mieog J, et al. Overexpression of a wheat α-amylase type 2 impact on starch metabolism and abscisic acid sensitivity during grain germination. Plant J. 2021;108(2):378–93.
54. Jia HF, Chai YM, Li CL, et al. Abscisic acid plays an important role in the regulation of strawberry fruit ripening[J]. Plant Physiol. 2011;157(1):188–99.
55. Luo H, Dai SJ, Ren J, et al. The role of ABA in the maturation and postharvest life of a nonclimacteric sweet cherry fruit[J]. J Plant Growth Regul. 2014;33:373–83.
56. Mita S, Suzuki-Fujii K, Nakamura K. Sugar-inducible expression of a gene for [beta]-amylase in Arabidopsis thaliana. Plant Physiol. 1995;107(3):895–904.
57. Liang G, Hou Y, Wang H, et al. VaBAM1 weakens cold tolerance by interacting with the negative regulator VaSR1 to suppress β-amylase expression. Int J Biol Macromol. 2023;225:1394–404.
58. Abdelfattah A, Whitehead SR, Macarisin D, et al. Effect of washing, waxing and low-temperature storage on the postharvest microbiome of apple. Microorganisms. 2020;8(6):944.
59. Strano MC, Altieri G, Allegra M, et al. Postharvest technologies of fresh citrus fruit: Advances and recent developments for the loss reduction during handling and storage. Horticulturae. 2022;8(7):612.
60. Mworia EG, Yoshikawa T, Salikon N, et al. Low-temperature-modulated fruit ripening is independent of ethylene in 'Sanuki Gold' kiwifruit. J Exp Bot. 2012;63(2):963–71.

Publisher's Note